Integrating Heat Sinks into a 3D Co-Design Network Model for Quick Parametric Analysis

Lauren M. Boteler[1], Steven M. Miner[2], Michael Fish[1], Morris Berman[1]
[1]U.S. Army Research Laboratory
Adelphi, MD, USA, 20783
Email: lauren.m.boteler.civ@mail.mil
[2]U.S. Naval Academy
Annapolis, MD, USA

ABSTRACT

Co-design and co-engineering have the potential to significantly advance the state of the art of electronics packaging. A key enabling capability of co-design are design tools which allow quick parametric design across various design spaces. ARL's ParaPower tool allows quick parametric thermo-mechanical design analysis of most rectilinear designs using a 3D thermal resistor network for both steady-state and transient heat loads. This work expands the ParaPower capabilities by allowing internal boundary cavity (IBC) features into the network structure. IBCs can be placed anywhere in the 3D rectilinear geometry and include two distinct boundary parameters: (1) a surface heat transfer coefficient and (2) an ambient temperature. Adding the IBC functionality to the network model significantly increases the design flexibility by permitting internal convection paths, non-rectilinear geometries, and heat sink geometry evaluation. This paper presents the IBC equations and illustrates the parametric capability by evaluating the effects of convection coefficient and heat sink material. The ability to quickly assess the thermal and stress effects of a wide variety of power module design parameters during the initial design process – with reasonable results and without the complexity of a full FEA analysis – can significantly improve the final design.

KEY WORDS: co-design, co-engineering, parametric study, thermal analysis, 3D network.

NOMENCLATURE

A	area, m^2
Q	heat generation, W
R	resistance, Ω
T	temperature, K
t	time, sec
c	specific heat capacity, J/K
V	volume, m^3
L	length, m
k	thermal conductivity, W/mK
h	heat transfer coefficient, W/m^2K

Greek symbols

ρ	density, kg/m^3
Δ	difference

Subscripts

0	node being solved for
i	neighboring node
∞	ambient
IBC	internal boundary cavity

Superscripts

p	timestep

INTRODUCTION

As electronics become smaller and more power dense, there is an increasing need for modeling tools which can quickly and accurately model the design space. ParaPower is a design tool which can quickly analyze parametric spaces including material types, material properties, layout designs, geometry, heat sink selections, and heat sink placement. Varying multiple parameters can quickly become computationally expensive for standard finite element analysis (FEA) and computational fluid dynamics (CFD) tools. ParaPower eliminates computer-aided design (CAD) in favor of numerical parameters that can be easily and quickly varied over a wide range. The tool is based on a resistor network which solves quickly in MATLAB, enabling fast, iterative thermal analyses and designs. A thermal resistor network is a foundation of thermal analysis and a 1D thermal resistance network is used by many thermal designers to determine steady-state temperatures. [1] ParaPower expands the 1D network into a 3D space with easily definable features which are further divided into elements. Each element has thermal resistors in all six directions from the center of the element, as is shown in Fig. 1.

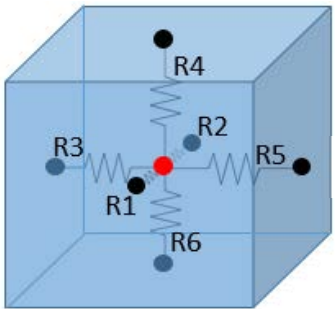

Fig. 1. Single node resistor network

ParaPower is based on an implicit Euler scheme solver to determine the temperature at each timestep. The implicit, or backward Euler method was selected due to its inherent stability. [2] The equation for a single node is given by:

$$\sum_{i=1}^{6}\left(\frac{1}{R_i}\left(T_i^{p+1}-T_0^{p+1}\right)\right)-CT_0^{p+1}=-Q_0-CT_0^{p}$$

$$\text{where}\qquad C=\frac{\rho_0^p c_0^p V_0}{\Delta t} \qquad (1)$$

Each element is then connected to each adjacent element forming a 3D thermal resistance network, as is shown in Fig. 2 for two dimensions. Each element creates an equation as shown above and the series of equations is solved through a matrix inversion in MATLAB to calculate the temperatures at the

center of each element. Fig. 2 is a representation of two features (yellow and blue) which have been divided into three elements each. The perimeter of the network model is comprised of ambient heat transfer coefficients (h_∞) and ambient temperature (T_∞) which can vary over the perimeter of the structure.

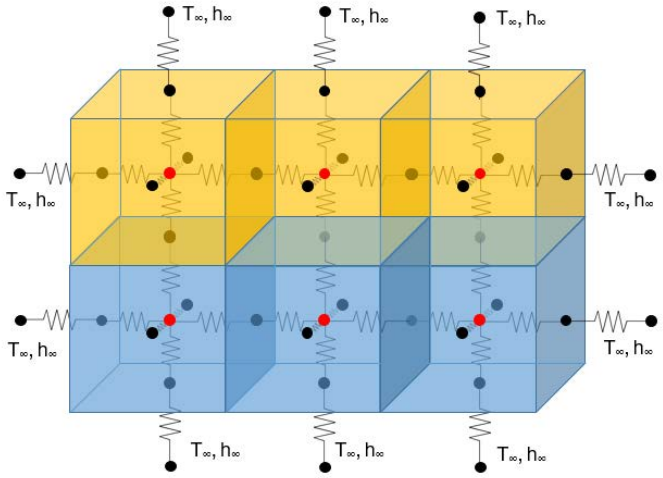

Fig. 2. Thermal Network Formulation

The model is adaptable to any number of features, heat loads, and heat transfer conditions.

In previous works [3, 4], Boteler and Miner demonstrated the implementation of a co-design approach using the ParaPower parametric analysis tool. The parametric analysis combined the thermal and CTE stress analyses providing an evaluation that addressed both aspects simultaneously. The analysis was applied to a typical planar type power module geometry and a novel high voltage stacked geometry. In these studies, comparison of temperatures to FEA analysis of the same geometry agreed to within 3°C and stresses agreed to within 30%. Run times for the network analysis were approximately 100 times faster than the FEA, not including the time required to generate the CAD model, and to verify mesh convergence and mesh independence. The current study extends the capability of ParaPower by including Internal Boundary Cavities (IBC's) which can be placed anywhere in the 3D rectilinear geometry. They are defined by two distinct boundary parameters: (1) a surface heat transfer coefficient and (2) an ambient temperature. Adding the IBC's permits inclusion of integrated heat sinks and non-rectilinear geometries.

MATHEMATICAL FORMULATION

IBCs are a way to put a break in the network and allow for convective heat transfer within the model and not just on the perimeter. Previous to this capability, the entire rectilinear geometry required solid elements. This significantly increases the design flexibility by permitting internal convection paths (Fig. 3), non-rectilinear geometries (Fig. 4), and heat sink geometry evaluation. Fig. 3 shows the ability to add a heat sink type structure by defining sections of the geometry as an IBC. This is equivalent to an air or liquid cooled heat sink with an ambient fluid temperature (T_{IBC}) and wall heat transfer coefficient (h_{IBC}).

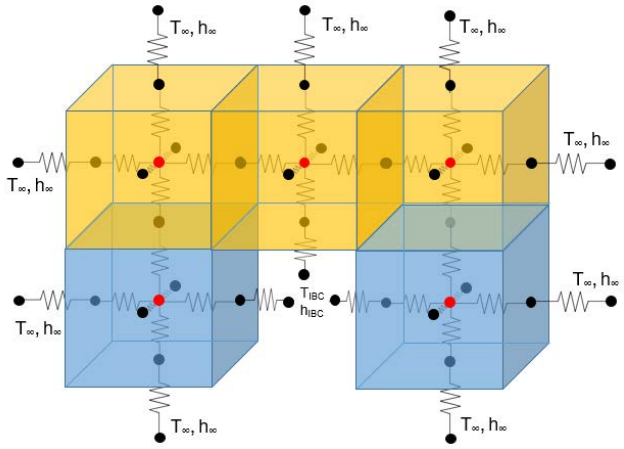

Fig. 3. Thermal network diagram showing an IBC used as a heat sink feature.

In addition, more complex non-rectilinear geometries can be used, as is depicted in Fig. 4. This could represent a chip on a substrate or component on a board that is surrounded by natural convection. Previously the network model required these elements to be solid but the IBC feature allows them to be defined as natural convection heat transfer features.

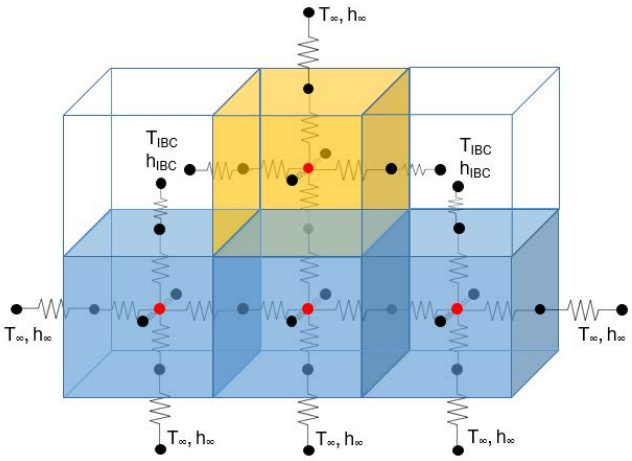

Fig. 4. Thermal network diagram including showing an IBC used to allow more complex geometries.

The IBCs can be placed anywhere inside the structure and do not have to be located on the perimeter wall as is shown in Figure 5 where the three sections in the middle represent IBCs.

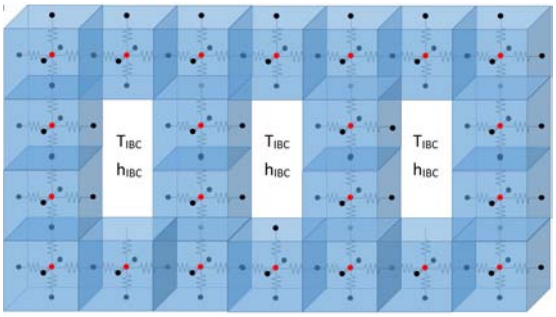

Fig. 5. Thermal network diagram depicting IBCs placed internal to the structure.

In the case of an internal resistor between any two solid nodes (*i* and *o*), the expression for the resistor, is given by Equation 2:

$$R_i = R_o = \frac{L_i}{2k_iA} + \frac{L_o}{2k_oA} \quad (2)$$

If node *i* is an ambient boundary node, the expression for the resistor is given by Equation 3:

$$R_i = \frac{1}{h_\infty A} + \frac{L_o}{2k_oA} \quad (3)$$

This same boundary formulation is used for an IBC, where the convection coefficient, h_{IBC}, is specified for that particular IBC. Equation 4 shows this.

$$R_i = \frac{1}{h_{IBC}A} + \frac{L_o}{2k_oA} \quad (4)$$

The overall approach and problem formulation do not change with the inclusion of IBC's. The change is simply to track whether a particular node is a solid, boundary or IBC node. In order to determine the effectiveness of the IBCs, a comparison with commercial finite element analysis (FEA) tools will be performed.

GEOMETRY

A basic heat sink geometry, shown in Fig. 6, illustrates the use of IBC's. The heat sink is an aluminum extrusion with 1.5 mm thick spreader plates top and bottom, separated by a series of fins that are 13 mm high by 0.5 mm thick that are on 2.0 mm centers. There is a 25 mm square area that is 0.5 mm thick centered on the top and bottom plates. A uniform heat flux of 100 W/cm^2 is applied to the outer surface of the squares shown in red on the figure, which represents heat dissipating components on both the top and bottom surfaces.

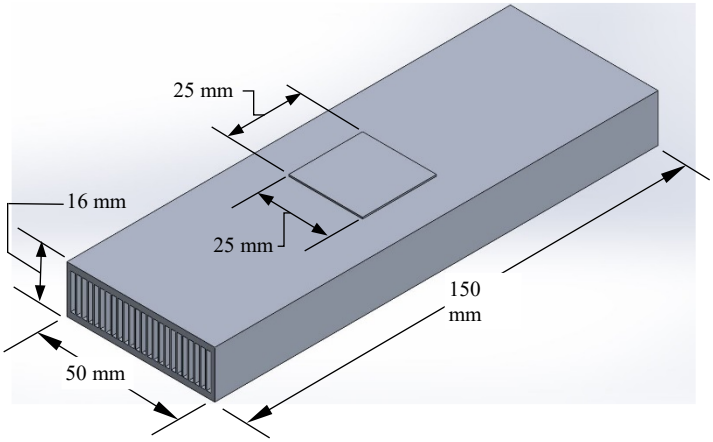

Fig. 6. Heat sink geometry used in the analysis

There are two symmetry planes in this model, one centered between the top and bottom spreader plates and one centered between the left and right sides of the heat sink. This geometry is modeled using both SolidWorks FEA and ParaPower. Temperatures from ParaPower are compared to the FEA results as a means of validation.

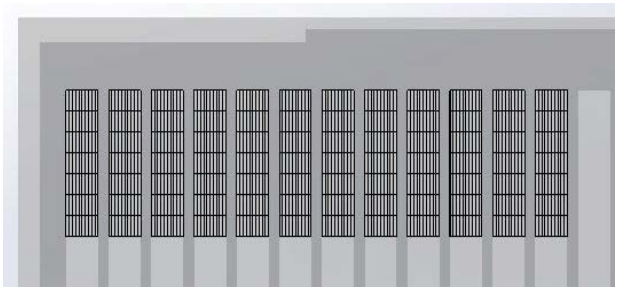

Fluid Mesh Front View

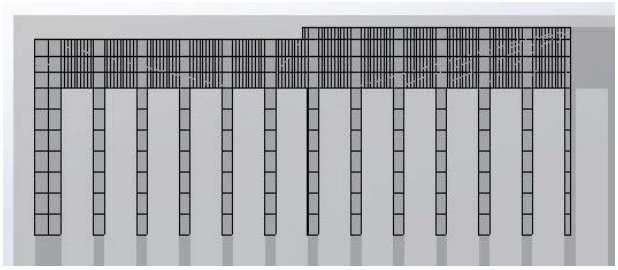

Solid Mesh Front View

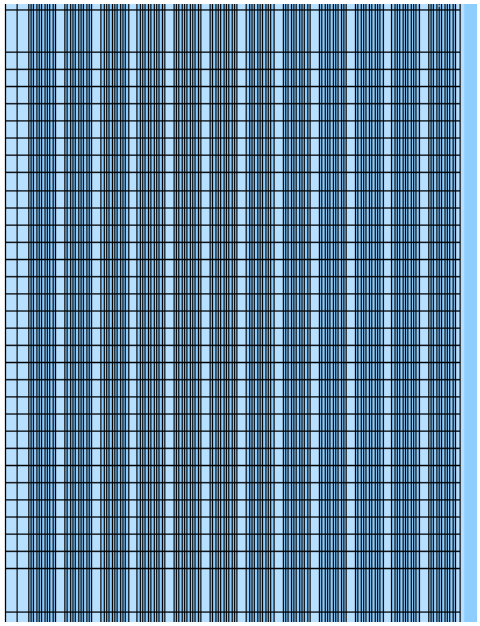

Solid / Fluid Mesh Top View

Fig. 7. Finite element analysis mesh

In addition to the geometry shown in Fig. 6, the FEA model includes upstream and downstream extensions. The extensions are 100 mm long upstream and 150 mm long downstream. They are made of a material with low conductivity, so as not to influence the temperature distribution in the heat sink. Both extensions have the same interior cross section as the heat sink without the fins. The extensions move the inlet and exit boundary conditions away from the actual heat

sink. At the inlet a fully developed velocity profile is used. At the exit a constant static pressure is specified. All walls are no-slip boundaries and the exterior surfaces are adiabatic. Fig. 7 shows the FEA mesh in the vicinity of the heat source. The mesh within the heat sink region, excluding upstream and downstream extensions, includes 85,000 fluid elements and 66,250 solid elements. The extensions add an additional 42,000 fluid and 31,700 solid elements.

Fig. 8 shows the grid used in ParaPower. It contains 3,500 nodes, of those 720 nodes are IBC's that represent the fluid channels in the heat sink and 370 nodes are the boundary nodes on the top surrounding the heat source.

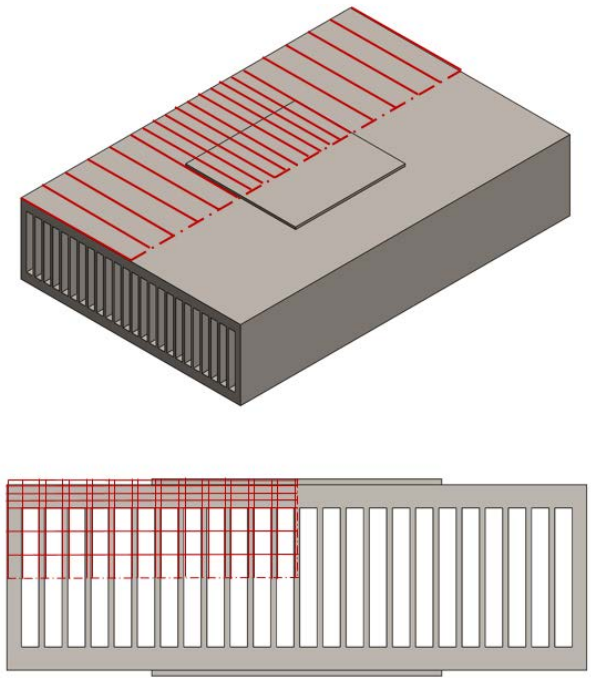

Fig. 8. ARL ParaPower Grid

RESULTS

Comparison of the FEA and ParaPower codes was done for a total flow rate of 0.8 kg/s of water through the heat sink. Based on the two symmetry planes the model flow rate was 0.2 kg/s, which results in a Reynold's number of 5000 based on the hydraulic diameter of the fin passages. The value of h used for the ParaPower run was 10,200 W/m^{2}K. Fig. 9 and Fig. 10 show the temperature comparisons for the heat source surface and the top surface of the heat sink, respectively. The ParaPower temperature values overlay the FEA temperature contours for both plots. Fig. 9 shows that the maximum temperature of the heat source for the two models agree to within 1 $^\circ$C. At the edges of the heat source the agreement is not as good, but is still within 5 $^\circ$C. Fig. 10 shows that for the top surface of the heat sink, the maximum temperature for the two models agree to within 2 $^\circ$C. Again, at the edges the agreement falls off to 5 $^\circ$C. The coarse mesh of the ParaPower model does not do as good a job of capturing the spreading and the removal of heat through spreader plate. However, the time to build and run the ParaPower model was 1/100th the time required for the FEA model. The execution time for ParaPower was 8 seconds versus 800 seconds for the FEA model.

Based on this comparison, ParaPower provides reliable results in a fraction of the time required for FEA. This makes it possible to perform parametric studies in a fraction of the time required for FEA. ParaPower allows a quick evaluation of design parameters.

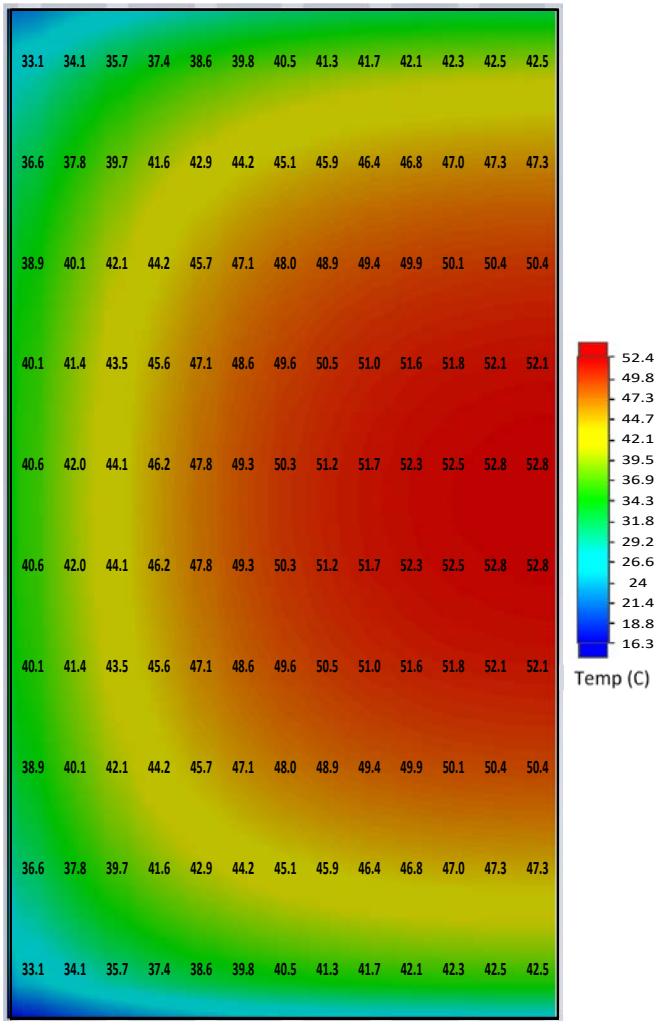

Fig. 9. Heat source surface temperatures with the ParaPower results superimposed on the FEA temperature plot.

As an illustration of ParaPower's parametric capabilityusing IBCs, three parametric studies were completed. Parameters varied included convection coefficient, h, spreader thermal conductivity, k, and spreader thickness.

The values of h varied from 2,000 W/m^{2}K to 50,000 W/m^{2}K. Table 1 lists the convection coefficients along with the corresponding Reynold's numbers and flow rates.

Table 1: Convection Coefficient Parametric Study

Flow Rate (kg/s)	*Re*	*h* (W/m^{2}K)
0.11	670	2000
0.34	2100	5000
0.8	5000	10000
2.5	15700	25000
6.0	37400	50000

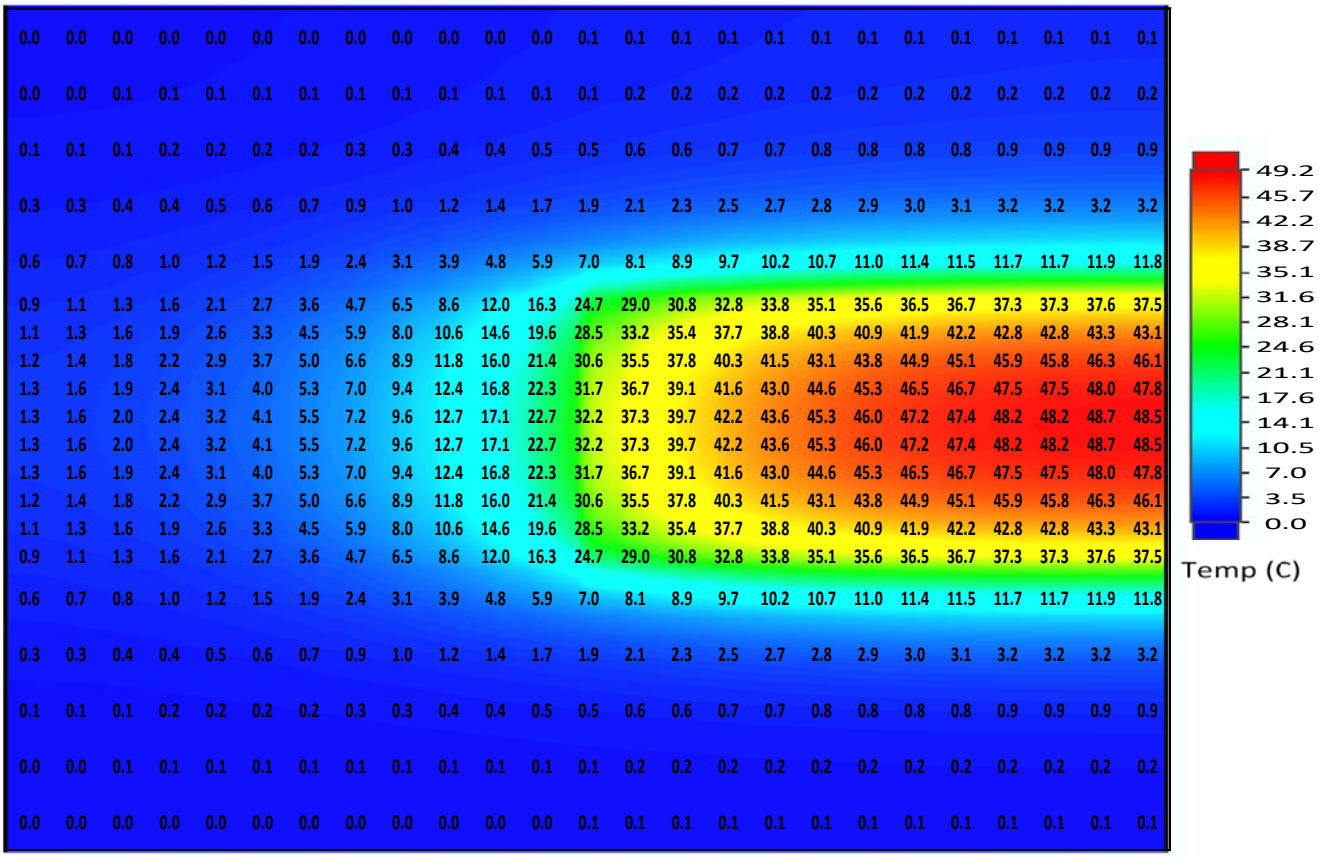

Fig. 10. Heat sink top surface comparison with the ParaPower results superimposed on the FEA temperature plot

The values of the heat spreader thermal conductivity, *k,* varied from 20 W/mK to 500 W/mK. Table 2 lists the values of conductivity and corresponding materials.

Table 2: Conductivity Parametric Study

Material	*k* (W/m K)
Stainless Steel	20
Brass	100
Aluminum	172
Copper	400
Silicon Carbide	500

The values of spreader thickness varied from 0.375 mm to 6 mm with values of 0.375 mm, 0.75 mm, 1.5 mm, 3.0 mm, 4.5 mm and 6.0 mm. In the following studies, the rise in source temperatures, ΔT's, were normalized by the component power dissipation such that the y-axis on the plots are in units of K/W. To determine the temperature rise, simply multiply the value by the power dissipation.

Fig. 11 shows the results for the convection coefficient study, which indicates that flow rates above 2.5 kg/s (h = 25,000 W/m^{2}K) provide only marginal reduction in maximum temperature. In addition, flow rates below 0.8 kg/sec (h = 10,000 W/m^{2}K) are in a very sensitive portion of the flow curve such that small fluxuations in flow rate could lead to large fluxuations in temperature. Operation between these two points is desirable.

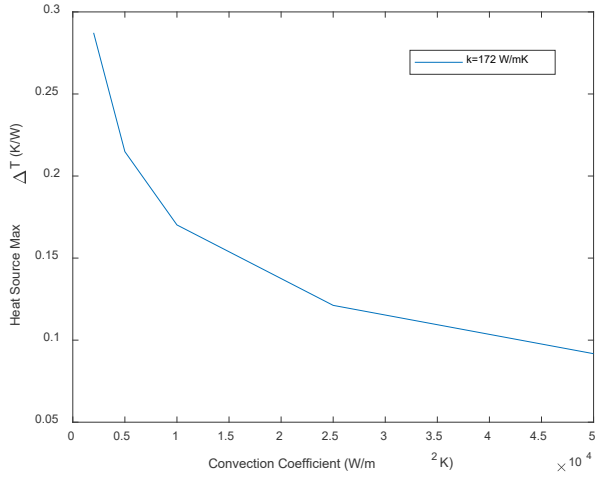

Fig. 11. Results of convection coefficient parametric analysis

Fig. 12 shows the results for the heat spreader parametric study, which varies both the thermal conductivity and convection coefficient for 30 simulations. For this study, the spreader thickness was set at 1.5 mm. The results show that moving to materials with thermal conductivities better than aluminum (k = 172 W/mK) provides little additional benefit, especially at higher convection coefficients.

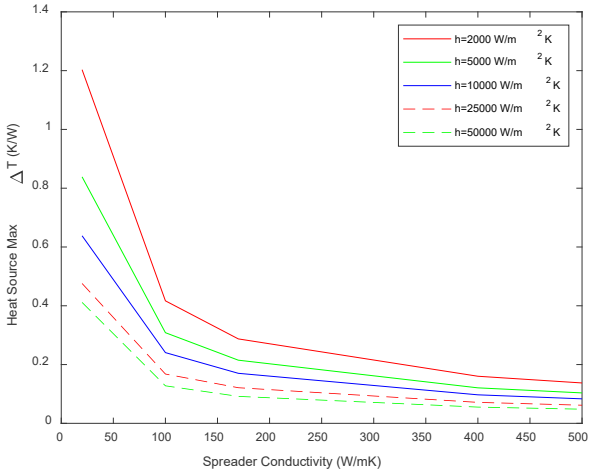

Fig. 12. Results of the heat spreader material conductivity parametric analysis.

The final study combined the effects of heat spreader thickness and convection coefficient over 30 simulations. Here the spreader conductivity was set at 172 W/mK. Fig. 13 shows the results for this study. It is interesting to note that for values of h less than 5,000 W/m^{2}K increasing the spreader thickness is beneficial. The additional thickness provides better spreading of the heat so that a larger portion of the heat sink is active in transferring the heat to the fluid. However, for values of h greater than 10,000 W/m^{2}K increasing the spreader thickness is detrimental. This is due to the increased thermal resistance caused by the added thickness, which acts to insulate the heat source from the fluid. It appears that at a value of h equal to roughly 7,000 W/m^{2}K the spreader thickness has no effect on the heat source maximum ΔT.

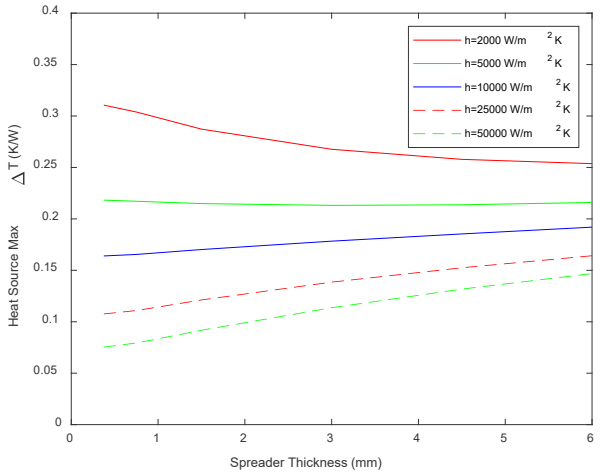

Fig. 13. Results of the heat spreader thickness parametric analysis

The time to complete the runs for the second and third parametric studies was 30 seconds, approximately 1 second per iteration. The results of the parametric studies drive the design towards a flow rate of around 2.5 kg/s, a spreader conductivity of at least 170 W/mK and a spreader thickness of 1.5 to 2.0 mm. Total time to run all of the parametric studies was less than 10 minutes, which included the time to set up the initial model geometry.

An example of the IBCs integrated into ParaPower is shown in Fig. 14 with the yellow sections representing the IBC features. The large yellow feature on the top is a natural convection boundary condition around the heated chip and on the surface of the heat spreader. The four yellow IBC features in the base represent heat sink flow channels.

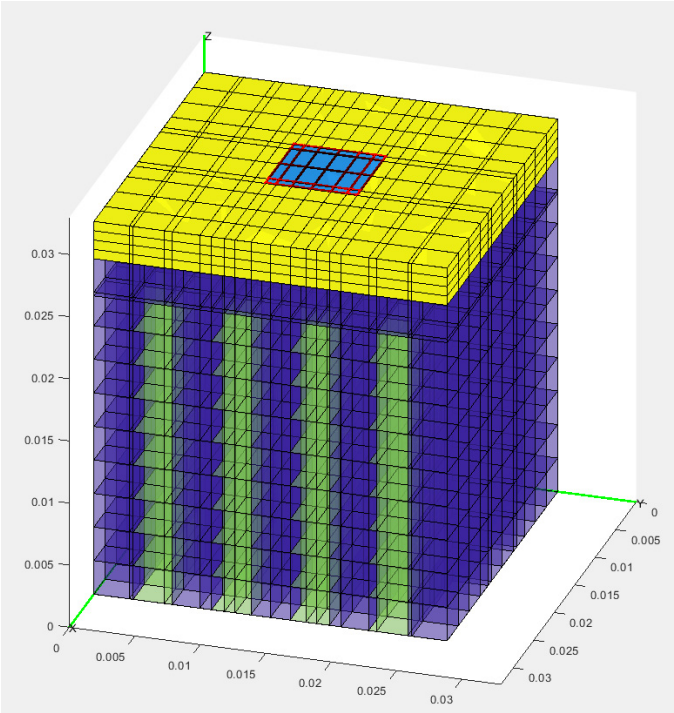

Fig. 14. ParaPower interface depicting integrated IBCs

Note that the current formulation of the IBC's restricts the temperature of these regions to specified fixed values. Meaning that the transfer of heat to a flowing fluid is not captured. There is no $\dot{Q} = \dot{m} c_p \Delta T$ capability, which would cause the temperature of the fluid to change according to the heat transferred to the fluid. This capability is currently being studied for implementation in the future. Inclusion of this linking between the heat transferred and the change in the fluid temperature will allow for more realistic analysis of heat sink designs.

CONCLUSIONS

The ability to model heat sink behavior was demonstrated through the inclusion of IBC's adds to ARL's ParaPower code. The ParaPower model was compared to FEA with maximum heat source temperatures agreeing to within 2ºC. In addition, several parametric studies were shown that demonstrate the usefulness of this low order modeling tool for quickly evaluating the design space and evaluating trade-offs between different design parameters. In order to more accurately capture heat sink behavior the inclusion of a heat capacity term that links the heat transfer to a corresponding change in fluid temperature is still needed.

ACKNOWLEDGEMENTS

The authors would like to thank the U.S. Army Research Laboratory, including Bruce Geil and Morris Berman, for supporting this work.

REFERENCES

[1] Incropera, Frank P., et al. *Fundamentals of heat and mass transfer*. Wiley, 2007.

[2] Anderson, Dale, John C. Tannehill, and Richard H. Pletcher. *Computational fluid mechanics and heat transfer*. CRC Press, 2016.

[2] L. M. Boteler and S. M. Miner, "Power packaging thermal and stress model for quick parametric analyses," in Proceedings of the ASME 2017 International Technical Conference and Exhibition on Packaging and Integration of Electronic and Photonic Microsystems InterPACK, pp. 1-8, 2017.

[3] L. M. Boteler and S. M. Miner, "Comparison of Thermal and Stress Analysis Results for a High Voltage Module Using FEA and a Quick Parametric Analysis Tool," in Proceedings of the ASME 2018 International Technical Conference and Exhibition on Packaging and Integration of Electronic and Photonic Microsystems InterPACK, pp. 1-10, 2018.